Available online at www.sciencedirect.com
SCIENCE DIRECT
Biochimica et Biophysica Acta 1757 (2006) 750–763
BIOCHIMICA ET BIOPHYSICA ACTA
BBA
www.elsevier.com/locate/bbabio

# Myoglobin with modified tetrapyrrole chromophores: Binding specificity and photochemistry

Stephanie Pröll [a], Brigitte Wilhelm [a], Bruno Robert [b], Hugo Scheer [a,*]

[a] Department Biologie I-Botanik, Universität München, Menzingerstr, 67, 80638 München, Germany
[b] Sections de Biophysique des Protéines et des Membranes, DBCM/CEA et URA CNRS 2096, C.E. Saclay, 91191 Gif (Yvette), France

Received 2 August 2005; received in revised form 2 March 2006; accepted 28 March 2006
Available online 12 May 2006

**Abstract**

Complexes were prepared of horse heart myoglobin with derivatives of (bacterio)chlorophylls and the linear tetrapyrrole, phycocyanobilin. Structural factors important for binding are (i) the presence of a central metal with open ligation site, which even induces binding of phycocyanobilin, and (ii) the absence of the hydrophobic esterifying alcohol, phytol. Binding is further modulated by the stereochemistry at the isocyclic ring. The binding pocket can act as a reaction chamber: with enolizable substrates, apo-myoglobin acts as a $13^2$-epimerase converting, e.g., Zn-pheophorbide *a'* ($13^2$S) to *a* ($13^2$R). Light-induced reduction and oxidation of the bound pigments are accelerated as compared to solution. Some flexibility of the myoglobin is required for these reactions to occur; a nucleophile is required near the chromophores for photoreduction (Krasnovskii reaction), and oxygen for photooxidation. Oxidation of the bacteriochlorin in the complex and in aqueous solution continues in the dark.


*Keywords:* Chlorophyll, transmetalated; Myoglobin binding site; Photochemistry; Stereochemistry, photosynthesis; Photodynamic therapy

## 1. Introduction

The two large groups of cyclic tetrapyrroles, the hemes (=Fe complexes) and chlorophylls (=Mg complexes) are in vivo bound to proteins. The protoheme (Fig. 1) containing myoglobin (Mb) and hemoglobin (Hb) were the first proteins for which crystal structures have been solved [1,2], and among the first proteins for which dynamic X-ray structures became available [3–7]. Based on the subsequently accumulated structural information, protoheme binding has been engineered successfully into synthetic proteins [8–10]. The small size, accessibility and solubility of, e.g., myoglobin or cytochrome *c* also rendered the heme proteins models which helped to develop basic concepts of protein structure and functions, including their energetic landscape and conformational space, by using the bound heme as a probe [11–13].

A variety of non-heme tetrapyrroles has been introduced into the myoglobin pocket. In view of a similar basic structure (Fig. 1), viz. a tetrapyrrole macrocycle with a coordinatively unsaturated central metal [14], it has been tempting to introduce chlorophyllous chromophores into the heme binding pocket. Objectives were to exploit some of the favorable properties like intense absorption in the vis-to-NIR spectral range and high fluorescence yield [15], and to investigate monomeric chlorophylls in a protein environment [16–18]. Hydrolysis of the long-chain esterifying alcohol is sufficient to render the pigment accessible to the heme binding sites of myoglobin [19] and hemoglobin [16]. Removal of the $13^2$-ester group and replacement of the central Mg by Zn has additionally been employed to improve binding and stability of the chromophore, respectively. Also accepted by the Mb binding pocket are linear tetrapyrroles with similar substitution pattern as protoheme (Fig. 1) [20–22]. Here, they adopt an all-Z-all-*syn* conformation that is chirally distorted but similar to that of protoheme [23–25].

*Abbreviations:* Apo-Mb, apo-myoglobin; BChl, bacteriochlorophyll *a*; BPheide, bacteriopheophorbide *a*; BV, biliverdin; Chl, chlorophyll *a*; Chlide, chlorophyllide *a*; Hb, hemoglobin; Mb, myoglobin; NaPB, sodium phosphate buffer; PCB, phycocyanobilin; Pheide, pheophorbide *a*; ProtoPheide, Proto-pheophorbide *a*; TFA, trifluoroacetic acid

* Corresponding author.
*E-mail address:* H.Scheer@lrz.uni-muenchen.de (H. Scheer).

0005-2728/$ - see front matter © 2006 Elsevier B.V. All rights reserved.
doi:10.1016/j.bbabio.2006.03.026

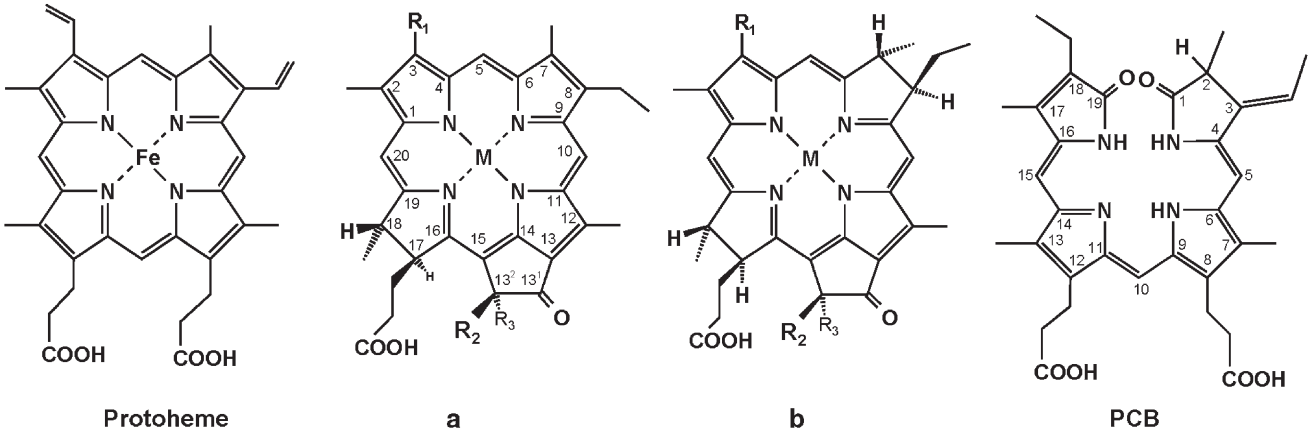


| Pigment | Formula | Metal | $R_1$ | $R_2$ | $R_3$ |
|---|---|---|---|---|---|
| $13^2$R-Zn-Pheide | a | Zn | $C_2H_3$ | H | $COOCH_3$ |
| $13^2$S-Zn-Pheide | a | Zn | $C_2H_3$ | $COOCH_3$ | H |
| $13^2$R-OH-Zn-Pheide | a | Zn | $C_2H_3$ | $COOCH_3$ | OH |
| $13^2$S-OH-Zn-Pheide | a | Zn | $C_2H_3$ | OH | $COOCH_3$ |
| $13^2$R-Zn-BPheide | b | Zn | $COCH_3$ | H | $COOCH_3$ |
| $13^2$S-Zn-BPheide | b | Zn | $COCH_3$ | $COOCH_3$ | H |
| [3-Acetyl]-$13^2$R- Zn-Pheide | a | Zn | $COCH_3$ | H | $COOCH_3$ |
| [3-Acetyl]-$13^2$S- Zn-Pheide | a | Zn | $COCH_3$ | $COOCH_3$ | H |
| Zn-Proto-Pheide* | a* | Zn | $C_2H_3$ | H | $COOCH_3$ |
| Zn-Pyro-Pheide | a | Zn | $C_2H_3$ | H | H |
| Zn-Pyro-BPheide | b | Zn | $COCH_3$ | H | H |
| Fe-Pheide | a | Fe | $C_2H_3$ | H | $COOCH_3$ |
| Ni-BPheide | b | Ni | $COCH_3$ | H | $COOCH_3$ |
| Pd-BPheide | b | Pd | $COCH_3$ | H | $COOCH_3$ |
| Pheide | a | - | $C_2H_3$ | H | $COOCH_3$ |
| BPheide | b | - | $COCH_3$ | H | $COOCH_3$ |
| Chl# | a | Mg | $C_2H_3$ | H | $COOCH_3$ |
| Chlide | a | Mg | $C_2H_3$ | H | $COOCH_3$ |

Fig. 1. Molecular structures of used chromophores. In cases where the $13^2$-configuration is not explicitly mentioned, the R-epimers are shown, which are usually more abundant. The nomenclature and numbering system used throughout is that recommended by the Joint Commission on Biochemical Nomenclature (JCBN) of the International Union of Pure and Applied Chemistry and International Union of Biochemistry (IUPAC-IUB) [73]. The recommended but cumbersome omission-resubstitution nomenclature is not used: substitutions are indicated by placing the modified group in square brackets [ ]; thus, 3-devinyl-3-acetyl-Chl *a* becomes [3-acetyl]-Chl *a*. The two sides of the tetrapyrrole plane are denoted α and β, indicating the bottom and top side, respectively, if the molecule is oriented as shown with the numbering running clockwise [73]. (★) Double bond between C17 and C18; (#) phytol at $C17^2$.

We became interested in chlorophyll binding to heme proteins in the context of their application to photodynamic therapy. Porphyrins with efficient intersystem crossing to the triplet state can be used to selectively attack tumors, bacteria or viruses after excitation with light. Among them, chlorophyll and bacteriochlorophyll derivatives have certain advantages like intense absorption in the therapeutic window and rapid biodegradation and/or excretion [26]. In the current work, such pigments were introduced into Mb to address two questions: (i) how do structural modifications of the pigments relate to their binding, and (ii) is the photoreactivity of the chromophore modified by binding to the protein, apo-Mb. We show that the presence of a central metal capable of binding extra ligand(s) is the most important feature, it even increases binding of open chain tetrapyrroles, and that in the myoglobin binding pocket, the chromophore is photochemically as active, or even more active, than in monomeric solution.

## 2. Materials and methods

### 2.1. Solvents and reagents

Acetone (AppliChem, Darmstadt, DE), toluene (Scharlau, Barcelona, ES), methanol (Baker, Deventer, GB), iso-propanol (Merck, Darmstadt, DE),

pyridine (Fluka, Buchs, CH), TFA (Merck, Darmstadt, DE) and glycerol (Roth, Karlsruhe, DE) were reagent grade and used without further purification. Reagent grade 3-butanone (Merck) was distilled before use. Sodium dithionite (Merck), sodium ascorbate (Sigma-Aldrich, Steinheim, DE) and zinc acetate (Merck) were used as supplied.

### 2.2. Pigments

BChl was extracted with methanol from freeze-dried cells of the carotenoid-less mutant G9 of *Rhodospirillum rubrum*. After evaporation of the solvent, the pigment was treated with trifluoroacetic acid (TFA) to yield crude BPheide [27], which was purified on silica gel plates (1.5% sodium ascorbate admixed) under Ar with toluene/acetone/methanol/iso-propanol (80:10:8:2 v/v/v/v) as eluent. $Zn^{++}$ was inserted into BPheide according to [28]. The resulting mixture of Zn–BPheide and BPheide (80/20) was directly used for reconstitution and irradiation experiments to minimize the formation of [3-acetyl]–Zn–Pheide during purification. If needed, the crude Zn–BPheide was chromatographed on silica gel plates as described above. The resulting pigment was >90% pure, and contained <10% [3-acetyl]–Zn–Pheide.

Chl was extracted from spray-dried *Spirulina platensis* (Behr Import, Bonn, DE) with methanol and purified according to [29]. It was treated with TFA [30] to yield Pheide, which was purified as described for BPheide. $Zn^{++}$ and $Fe^{++}$ were inserted into Pheide according to [31]. The resulting mixtures of M-Pheides (Fig. 1) and Pheide (80/20) were directly used for reconstitution to minimize the formation of $13^2$-OH-derivatives. $13^2$-OH–Zn–Pheide was produced by leaving an aerated solution of Zn–Pheide in methanol in the dark at ambient temperature for 3 days [32,33]. It was purified by HPLC (μBondapak™ C18, 125 Å, 10 μm, 19×30 mm; Waters, Milford, USA) with aqueous sodium acetate (25 mM)/acetone as gradient eluent (50/50 ($t$=0–10 min), 46/54 ($t$=20 min), 42/58 ($t$=30 min), 38/62 ($t$=50 min), 20/80 ($t$=70 min), 0/100 ($t$=80 min)). Pd–BPheide was a gift of Negma (Paris, FR). Chlide was prepared according to [34]. Ni–BPhe was prepared according to [28], and subsequently hydrolyzed by TFA-treatment (see above) to yield Ni–BPheide, which was purified on silica gel plates. Protopheophorbide *a* (Protopheide) and [Zn]-Protopheide were prepared according to Helfrich et al. [31]. PCB was extracted from *Spirulina platensis* and purified as described by Storf et al. [35].

### 2.3. Preparation of apo-Mb

The apoprotein of horse heart myoglobin (Mb) (Sigma-Aldrich, München, DE) was prepared according to published procedures [36]. Hemin was extracted by the acid–butanone procedure [36], followed by dialysis against deionized water, an aqueous solution of sodium hydrogen carbonate (0.6 mM) and finally Tris/HCl buffer (10 mM, pH 8.3) [17]. After purification over a DEAE-cellulose column (Whatman, Maidstone, UK) in Tris/HCl (10 mM, pH 8.3) the solution was concentrated by the use of centrifugal filter devices (Amicon-10 kDa, Millipore, Bedford, MA, USA), dialyzed exhaustively against doubly deionized water, and lyophilized.

### 2.4. Pigment insertion

All reconstitution steps were done under Ar and dim green light. A 1.5- to 3-fold molar excess of pigment was dissolved in pyridine, mixed with the same volume of sodium phosphate buffer (NaPB) (10 mM, pH 6.3) and slowly added to apo-Mb (1%) in the same buffer under rapid stirring at 4 °C. The final pyridine concentration was 5%. After further stirring for 15 min, the mixture was applied to a column of Sephadex-G-25-medium (Amersham-Pharmacia, Freiburg, DE) equilibrated with NaPB (10 mM, pH 6.3). The intensely pigmented band which eluted was dialyzed against the same buffer over night at 4 °C, and then bound to a column of CM-Sepharose-CL-6B (Amersham-Pharmacia) equilibrated with the same buffer. The complex eluted as a single band, when developed with a continuous NaPB gradient (10–100 mM, pH 6.3–7.8). The resulting solution of the pigment protein complex (0.1–0.2 mM, 60–95% yield, determined spectrophotometrically) was stored under Ar at 4 °C.

To enhance the solubility of Pd–BPheide and (B)Pheide, the reconstitution step with these pigments was additionally done in NaPB (10 mM, pH 6.3) containing 0.1% (v/v) Triton-X-100, 2 mM EDTA and 1 mM β-mercaptoethanol. The general reconstitution procedure was also slightly modified in case of PCB. A 1.5- to 3-fold molar excess of pigment was dissolved in pyridine, mixed with the same volume of deionized water containing a 10-fold excess of zinc acetate and equilibrated for 5 min. The solution was then slowly added to apo-Mb (1%) in NaPB (10 mM, pH 6.3) under rapid stirring at 4 °C. After further stirring for 15 min, the blue solution was centrifuged to remove precipitated excess pigment, protein and zinc phosphate, and the supernatant applied immediately to a column of Sephadex-G-25-medium (see above). The green pigmented band which eluted was dialyzed against NaPB (see above). As the complex is rather labile under ion-exchange conditions, the 2nd chromatography over CM-Sepharose-CL-6B was omitted. The pigment-protein was purified instead by native PAGE (see below).

### 2.5. Sample preparation

Aliquots from stock solutions of the pigment protein complexes were diluted with NaPB (10 mM, pH 6.3) to an absorbance of 0.5 at the $Q_y$-maximum (1 cm path length), corresponding to concentrations of 7.8 to 8.8 μM depending on the pigment. The final volume was 2 ml. Free pigments were either dissolved in 5 μl pyridine and then diluted with the same buffer, or directly dissolved in the appropriate solvent to a final volume of 2 ml with an absorbance of 0.5 at the $Q_y$-maximum. In case of irradiation experiments under anaerobic conditions, buffer and solvents were degassed and flushed with Ar before use.

### 2.6. Irradiations

A 150 W cold light source (Intralux 150 H Universal, Volpi, Zürich) equipped with a 630 nm low-pass filter (RG 630, Schott) was used for irradiation. The light intensity was 900 μmol photons $m^{-2}$ $s^{-1}$ at the surface of the cuvette. The solutions were irradiated for 1, 3, 10 and 20 min at ambient temperature in 1 cm glass cuvettes. The progress of the reaction was monitored by absorption spectroscopy. For aerobic photoreactions, the samples were magnetically stirred during illumination under air. For anaerobic photoreactions, the solvents were degassed for 10 min and regassed with argon by flushing them for 15 min with Ar. The pigment or pigment protein complex was then added to the deaerated solvent, introduced into Thunberg cuvettes, and deaerated again by 10 pump/Ar-gassing cycles. This procedure does, however, not result in complete deaeration of the samples. Illumination in the presence of a reductant (sodium dithionite, 5 mg) was done according to the Ar-protocol, and the reductant added under Ar in the Thunberg cuvettes immediately before the irradiation.

### 2.7. Pigment extraction

Aqueous solutions of the Mb-complexes and their photoproducts were cooled to 4 °C and treated three times with ice-cold 3-butanone. Care was taken that the extraction is exhaustive. If there was any remaining pigment, the procedure was repeated. The organic phase was evaporated under vacuum and the pigments stored under Ar at −20 °C until HPLC analysis. After irradiation of pigments in organic solvents, the latter were evaporated and the pigments were stored the same way.

### 2.8. HPLC of photobleaching products

Zn–(B)Pheide-derivatives were analyzed by HPLC (Grom-Sil 120, ODS-4, HE, 5 μm, 250×4.6 mm; Grom, Herrenberg-Kayh, DE) and gradient elution with a mixture of aqueous sodium acetate (25 mM) and acetone (50/50 ($t$=0 min), 38/62 ($t$=23 min), 0/100 ($t$=29 min)). The HPLC unit consisted of a pump and control device (600E multisolvent/delivery system, Waters), an in-line degasser (Waters), and a diode array spectrophotometer (Tidas, J&M, Aalen, DE). All solvents were flushed with He.

### 2.9. Spectroscopy

A double beam UV-Vis-near-infrared spectrophotometer (UV 2401 PC, Shimadzu) was used to measure steady state absorption spectra. CD-spectra were

taken with a Dichrograph CD6 (Jobin-Yvon, Grasbrunn, DE) using a R 374 photomultiplier (Hamamatsu, 300–800 nm). Mass spectrometric analyses were carried out on a Q-TOF-I hybrid mass spectrometer (Micromass, Manchester, GB) equipped with an orthogonal nano-electrospray ionization source operating in the positive electrospray ionization mode. NMR spectra were recorded at 300 K on a DRX 600 spectrometer (Bruker, Karlsruhe, DE) in 75% NaPB (10 mM, pH 6.3)/ 25% $D_2O$.

### 2.10. Resonance Raman spectra

The spectra were obtained at 77 K in a SMC-TBT flow cryostat using a U1000 Raman spectrophotometer (Jobin-Yvon, Longumeau, FR) equipped with a $N_2$-cooled, back-thinned CCD detector (Spectrum One, Jobin-Yvon), as described previously. Excitation was provided by an Innova 100 Argon laser (457.9 and 488.0 nm, Coherent, Santa Clara, CA, USA) an Innova 90 Krypton laser (406.7 and 413.1 nm, Coherent) or a Helium-Cadmium laser (441.6 nm, Liconix, Santa Clara, CA, USA). During the experiments, the power of the laser beam reaching the sample is less than 1 mW. Combination of using such a low power, and working at cryogenic temperatures inhibits pigment degradation during the Raman measurements. Chemical degradation of the sample usually results either in the appearance of new bands in the signal, or in the appearance of an increasing fluorescence background; none of these were observed during the Raman measurements.

### 2.11. Native gel electrophoresis

Further analyses of the pigment protein complexes were carried out in a continuous native gel system (Mini-Protean II Dual-Slab Cell and Constant Voltage Power Supply 1000/500, Bio-Rad, München, DE). The gels contained 10% acrylamide (rotiphorese® Gel 30, 29.2:0.8% w/w acrylamide:bisacrylamide, Roth) and no detergent. The samples were concentrated in NaPB (10 mM, pH 6.3) by the use of centrifugal filter devices (see above), mixed with the same volume of glycerol and immediately applied to the gel. Electrophoresis was done with 150 V for 1.5 h in dim green light with Tris/glycin buffer (626 mM Tris/HCl, 192 mM glycin, pH 8.3).

Preparative scale gel electrophoresis was done analogously by using vertical electrophoresis cells (PROTEAN II xi/XL, Bio-Rad) at 10 °C. The preparative gels were developed for 1 h with 15 W and then for 11.5 h with 8 W. Elution of the single bands was done by rapid stirring of the crushed gel band in NaPB (10 mM, pH 6.3) under Ar for 2 h at ambient temperature. The resulting solution was filtered, concentrated (see above) and further cleaned by applying it to a PD-10 column (Amersham-Biosciences, Uppsala, SE) in NaPB (10 mM, pH 6.3). If necessary, the gels were stained with Coomassie-Blue.

## 3. Results

### 3.1. Specificity of pigment binding

Pigment incorporation into apo-Mb was studied under standardized conditions with different (B)Chl-derivatives, and the linear tetrapyrrole, phycocyanobilin (PCB) (Fig. 1). Several structural features were tested for their influence on pigment binding. A characteristic difference between chlorophylls and hemes is the presence of the isocyclic ring in the former. Previous studies had shown, that this ring does not interfere with binding [37]. However, an asymmetric center is generated in the isocyclic ring (C-$13^2$). We therefore first investigated the influence of the $13^2$-stereochemistry on binding. The $13^2$R-epimers of both Zn–Pheide and Zn–BPheide, are readily incorporated into the heme binding pocket of Mb. The resulting complexes are formed in good yields and elute as single green bands from the ion-exchange column. They have similar absorption (Table 1), CD (Table 2) and $^1$H-NMR (Fig. 2) features as described previously [37] for the complexes of the respective pyro-derivatives lacking the $13^2$-substituent (Fig. 1). They both move as distinct green bands when applied to native gel electrophoresis, this is the method of choice to obtain the complexes in pure form (Fig. 3).

The $13^2$S-epimers of Zn–Pheide and Zn–BPheide do also form complexes with apo-Mb, but only transitorily. Reconstitution of apo-Mb with an excess of epimeric mixtures (R/S = 3/1) of Zn–Pheide (Fig. 4) or Zn–BPheide (Fig. 5), results in protein complexes that contain only the respective R-epimers: the pigments

Table 1
Absorption spectra of (bacterio-)chlorophyll derivatives in acetone solution and of their myoglobin complexes. Values in brackets refer to transiently formed complexes (see text)

| Pigment | Solution (acetone) | | | Mb-complex (buffer) | | |
|---|---|---|---|---|---|---|
| | $Q_y$ $\lambda_{max}$ [nm] | Soret $\lambda_{max}$ [nm] | Ratio $A_Q/A_{Soret}$ | $Q_y$ $\lambda_{max}$ [nm] | Soret $\lambda_{max}$ [nm] | Ratio $A_Q/A_{Soret}$ |
| $13^2$R–Zn–Pheide | 656 | 425 | 0.74 | 661 | 436 | 0.73 |
| $13^2$S–Zn–Pheide | 656 | 425 | 0.74 | (661) | (436) | (0.73) |
| $13^2$(R/S)–OH–Zn–Pheide | 656 | 425 | 0.74 | 660 | 435 | 0.75 |
| $13^2$R-Zn–BPheide | 763 | 354 | 0.93 | 774 | 362 | 1.15 |
| $13^2$S-Zn–BPheide | 763 | 354 | 0.93 | (774) | (362) | (1.15) |
| 3-Acetyl-$13^2$R–Zn–Pheide [a] | 675 | 429 | 0.92 | 680 | 432 | 0.52 |
| 3-Acetyl-$13^2$S–Zn–Pheide [a] | 675 | 429 | 0.92 | (680) | (432) | (0.52) |
| Fe-Pheide | 684 [b] | 387 [b] | 0.25 | 658 | 424 | 0.43 |
| Ni–BPheide | 778 | 336 | 1.05 | 775 | 346 | 1.17 |
| Pd–BPheide | 754 | 331 | 1.56 | – | – | – |
| Pheide | 666 | 410 | 0.46 | – | – | – |
| BPheide | 747 | 358 | 0.47 | – | – | – |
| Chl | 663 | 430 | 0.74 | – | – | – |
| Chlide | 663 | 430 | 0.74 | 664 | 436 | 0.80 |
| Zn-Pyro-Pheide [c] | | | | | | |
| Zn-Pyro-BPheide [c] | | | | | | |
| PCB | 689 [d] | 375 [d] | 0.78 [d] | 737 | 379 | 0.43 |

[a] Absorbance values are taken from of a mixture with Zn-BPheide *a*.
[b] Broad bands in acetone.
[c] From [37].
[d] In methanol/HCl.

Table 2
CD-data of Mb complexes with $13^2$-carbomethoxy-Zn–Pheide complexes (left, this work) and the analogous Pyro-Zn–Pheide complexes (right, data taken from [37])

| Complex | $13^2$-carbomethoxy-derivative | | Pyro-derivative | |
|---|---|---|---|---|
| | $\lambda_{max}$ [nm] | $\Delta A \times 10^5$ | $\lambda_{max}$ [nm] | $\Delta A \times 10^5$ |
| Zn–Pheide–Mb | 666 | +16.5 | 661 | +7.8 |
| | 606 | +2.8 | 612 | +2.0 |
| | 411 | +26.6 | 440 | +8.3 |
| Zn–BPheide–Mb | 774 | +16.0 | 780 | +6 |
| | 587 | +4.6 | 591 | +12 |
| | 392 | +29.8 | 396 | +23 |

extracted from these complexes were >95% R-configured, while the S-epimers and excess R-epimers were not bound to the protein and retained on the gel filtration column. The small amounts (<5%) of the S-epimers in Figs. 4, 5 are due to slow epimerization during extraction and analysis. If $13^2$R/S epimer-mixtures of Zn–Pheide or Zn–BPheide were used for reconstitution with a 2-fold excess of apo-protein, the complexes finally formed are again those of the $13^2$R-epimers. Obviously, the enrichment of the $13^2$R-epimer is therefore not due to a mere preference of apo-Mb, but involves an accelerated epimerization. HPLC-analyses of the pigments extracted from these complexes are shown in Table 3. In solution, the epimerization of the bacteriochlorin complex is much slower than that of the chlorin complexes [32]. We also did observe such a difference in the Mb-complexes. For the chlorin, the reaction in solution depends both on the concentration and the solvent [38], but in the complex, it is much faster than the fastest reactions observed in solvents. Epimerization proceeds via enolization, and therefore requires an acidic H-atom in position C-$13^2$. Enolization is therefore inhibited in the $13^2$-hydroxy-derivatives. In this case, both the R- and S-epimers are accepted by the Mb-pocket (Table 2), which seems to argue against a directing influence of the C-$13^2$-stereochemistry. However, a certain preference is indicated by the observation that only $13^2$S–OH–Zn–

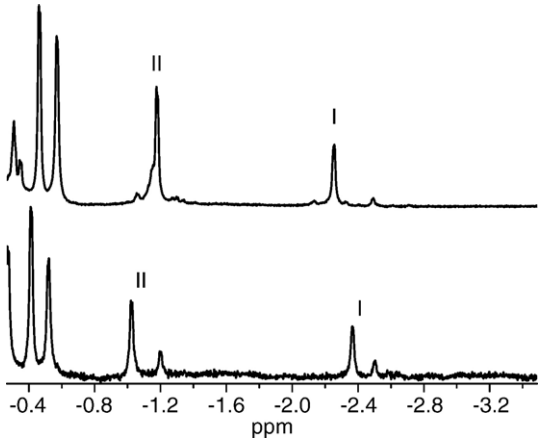


Fig. 2. $^1$H-NMR-spectra of Zn–Pheide–Mb (bottom) and Zn–BPheide–Mb (top) in NaPB (10 mM, pH 6.3 and 25% $D_2O$). Zn–Pheide–Mb and Zn–BPheide–Mb. I and II denote protein signals of Val68 that are high-field shifted by the tetrapyrrole ring-current (see text).

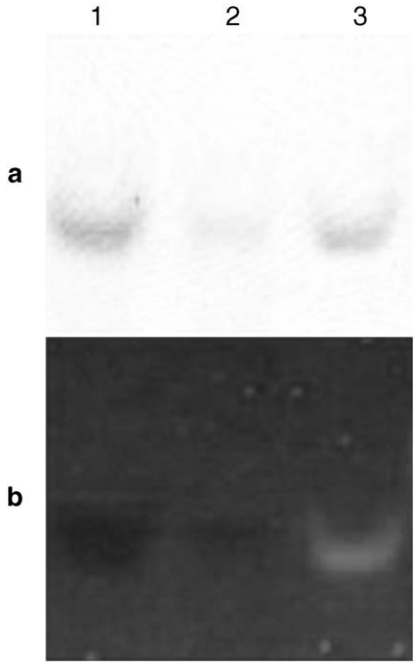


Fig. 3. Native PAGE of Fe–Pheide–Mb [1,2] and Zn–PCB–Mb [3]. Panel a shows the native, unstained complexes, panel b shows the complexes under fluorescence conditions ($\lambda_{exc}$=360 nm).

Pheide (α-oriented $13^2$-$COOCH_3$) is formed during illumination of Zn–Pheide–Mb.

The chlorophyll derivatives used for reconstitution are conformationally more demanding than the native Mb ligand, Fe-Protoporphyrin. In all (bacterio)chlorophyll derivatives used, the propionic acid bound to the $sp^3$-hybridized C-17 protrudes from the macrocycle plane to the β (=top) side of the macrocycle (for definition of the diastereotopic "faces" of the tetrapyrrole plane see legend Fig. 1), while it is oriented equatorially at the $sp^2$-hybridized C-17 in protoheme. However, in native Mb, this heme side-chain is bent upward [39] (Fig. 6), similar to the situation in chlorophylls,

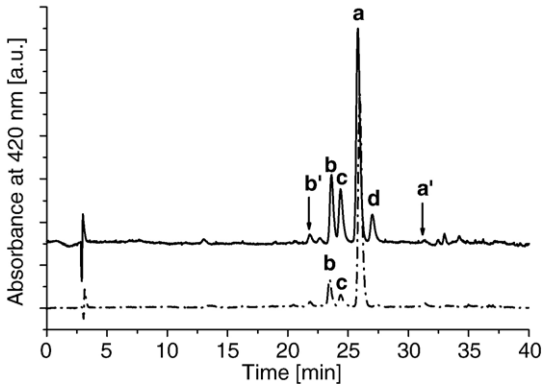


Fig. 4. HPLC-chromatograms of Zn–Pheide and derivatives extracted from Zn–Pheide–Mb before (–·–·–) and after (—) irradiation of the pigment protein complex for 20 min. Variations in the retention times of the same product due to varying solvent temperature and varying column states at different days were manually equalized. Pigments were identified by co-chromatography with authentic products: **a**=$13^2$R-Zn–Pheide *a*, **a'**=$13^2$S-Zn–Pheide *a*, **b**=$13^2$S-OH-Zn–Pheide *a*, **b'**=$13^2$R–OH–Zn–Pheide *a*, **d**=Zn-Proto-Pheide *a*. The structure of product **c** ($m_c$=686 g/mole) is not known.

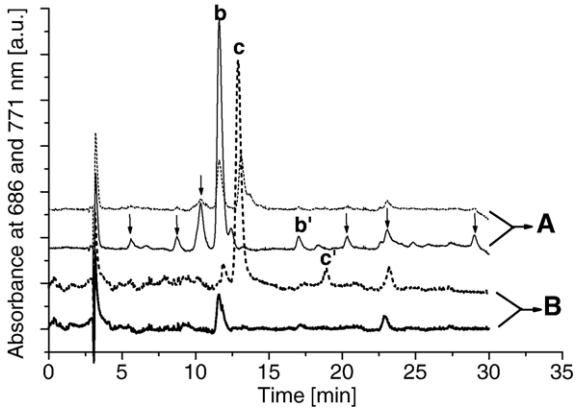


Fig. 5. HPLC-chromatograms of Zn–BPheide and derivatives extracted from Zn–BPheide–Mb before (**A**: 766 nm, 686 nm) and after (**B**: 686 nm; 766 nm) irradiation of the pigment–protein complex for 20 min. Pigments were identified by co-chromatography with authentic products: **b**=13$^2$R-Zn–BPheide, **b'**=13$^2$S-Zn–BPheide, **c**=3-acetyl-13$^2$R–Zn–Pheide (=oxidized Zn–BPheide, double bond at C7/C8), **c'**=3-acetyl-13$^2$S–Zn–Pheide. Products labeled with an arrow were not identified, they all show bacteriochlorin-type spectra and their intensities vary from extraction to extraction.

which may be an important factor that the latter are also accepted by Mb. The equatorially located 13-propionic acid side chain is also bent out-of-plane in native Mb, but in this case to the α (=bottom) side of the macrocycle. This substituent is missing in the pyrochlorophyll derivatives studied before in myoglobin [37], but there is a comparable substituent (13$^2$-COOH$_3$) in the pigments used in this study (Fig. 1). In the 13$^2$R-configured Chl and BChl derivatives, this polar, sterically demanding group is protruding to

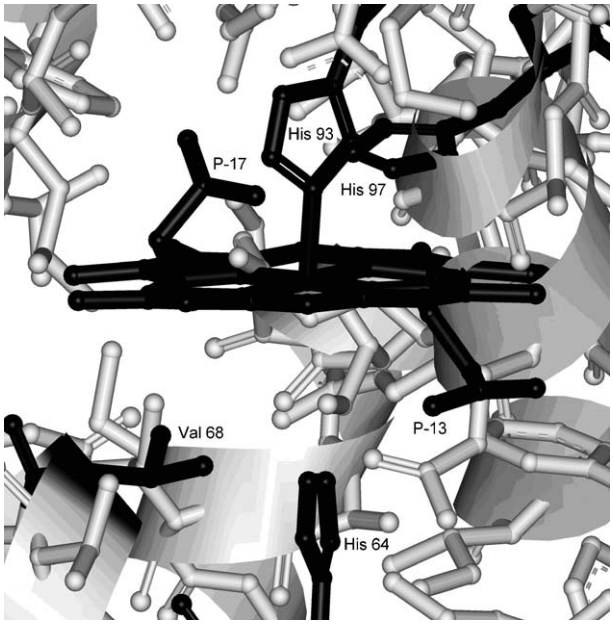


Fig. 6. Illustration of the heme environment and the conformation of the propionic acid side chains in the horse heart Mb binding pocket. View into the pocket along the tetrapyrrole plane, with the propionic acid side chains P-13 (attached to C-13) and P-17 (attached to C-17) near the viewer. Amino acid residues His97, His93, His64 and Val68 are rendered prominent, the complexed azide is not shown (pdb entry 1AZI).

Table 3
Percentage of R-epimers of several pigments analyzed by HPLC before and after formation of the pigment protein complex

| Pigment | Percentage of R-epimer | | |
|---|---|---|---|
| | Before | 1 h | 24 h |
| Zn–Pheide | 66% | 92% | 98% |
| 13$^2$-OH–Zn–Pheide | 25% | 25% | 25% |
| Zn–BPheide | 43% | 46% | 63% |
| 3-Acetyl–Zn–Pheide | 50% | 94% | 95% |

the α (=bottom) side of the macrocycle, in an orientation similar to that of the carboxylate group of the 13-propionic acid of heme in Mb (Figs. 1, 6). In the 13$^2$S-epimer, it exchanges its position with the 13$^2$-H and is now located at the β (=top) side, which apparently renders binding more difficult. This concept of steric hindrance in controlling binding, is also supported by results obtained with the epimeric 13$^2$-OH–Zn–Pheides. Here, the size-difference between the two 13$^2$-substituents (OH, COOCH$_3$) is less pronounced, and now both epimers are accepted by the binding pocket (Table 1).

In contrast to the phytol-lacking Chlide, its in vitro precursor Chl was not accepted by apo-Mb into its heme binding pocket. The large, hydrophobic phytol residue (C$_{20}$H$_{39}$O) seems to hinder the incorporation, whereas modifications of the substituents at C-13$^2$ (see above) and C-3 (Fig. 1) do not inhibit the pigment binding. These results are in accordance with the literature [37,40].

The next factor tested was the central metal. Mg and Zn were the only central metals that had been tested before for binding [17]. We also found that Mb-complexes are formed in good yields with Chlide and Zn–Pheides, their absorptions match those given by Wright and Boxer [37]. Reconstitution of apo-Mb was also possible with Fe-Pheide and Ni–BPheide. The latter forms complexes in yields comparable to the Zn-complexes, the main absorptions are given in Table 1. Fe–Pheide–Mb is only formed in very low yields, but we ascribe this to the poor solubility of the monomeric pigment in the reconstitution system, where Fe-Pheides tend to form μ-oxo-dimers [41] which are too big for the Mb-pocket. Most of the pigment therefore remains bound to the column under the workup-conditions of the complexes. The eluting Mb complex migrates as a grayish-green band in native gel electrophoresis[1] (Fig. 3), with absorption maxima at 658 and 424 nm (Table 1). Neither Pd–BPheide, nor the metal-free BPheide or Pheide could be incorporated into the Mb pocket under the standard conditions used for reconstitution. These pigments aggregate readily, but even if the reconstitution buffer was modified (see Materials and methods) to keep these pigments monomeric, no pigment-Mb-complexes could be isolated by chromatography or gel electrophoresis. A control experiment with Zn–(B)Pheide resulted in complexation with Mb in good yields. A distinct

[1] We used native polyacrylamide gel electrophoresis to further purify the pigment–protein-complexes and as a test for pigment incorporation. A surprising and still unexplained result of these studies was the observation of satellite bands for all complexes investigated, with the only exception of apo-Mb. NMR-, mass, and absorption-characteristics of the satellites were the same as for the respective main bands.

difference between Pd and the other metals is its coordination chemistry: while Mg, Zn, Ni and Fe can coordinate extra ligands, Pd is coordinatively saturated in the tetrapyrrole [28]. Like the metal-free pheophorbides, it therefore does not bind an extra ligand. The capacity of binding extra ligand(s) therefore appears to be essential for binding. This is supported by binding experiments with the linear tetrapyrrole, phycocyanobilin (PCB). It was not bound to Mb under the reconstitution conditions. However, if Zn-acetate is added to a pyridine–water solution of PCB prior to reconstitution, the pigment is complexed by the protein. After removal of the surplus of blue pigment, the remaining green complex is stable on native gels where it moves as a green band that shows an orange-red fluorescence (Fig. 3). Free PCB is non-fluorescent, but fluorescence is induced by incubation with $Zn^{2+}$ [42]. The induction of fluorescence in the Mb-complex then supports binding of the chromophore as a Zn complex. An additional indication for the complexation of PCB as a Zn-complex is the strongly red-shifted absorption of its long wavelength band. A similar shift was observed by Falk et al. [23] upon Zn-chelation of the biliverdin–Mb complex.

### 3.2. Characterization of the Zn–(B)Pheide–Mb–complexes

As reported before [37] for the Zn– and Mg–pyro-(B)Pheides, binding of most pigments tested resulted in red-shifted absorption maxima, as compared to those in acetone solution (Table 1). The shift of the $Q_y$-absorption amounts to 1–11 nm, with the exception of the Fe- and Ni-complexes which gave small (Ni) and pronounced (Fe) blue-shifts of 3 and 27 nm, respectively. In the Soret region, the protein induces red-shifts in all pigments tested (Table 1).

The $^1$H-NMR-spectra of Zn–Pheide–Mb and Zn–BPheide–Mb show similar features in the high-field region (Fig. 2) as were described by Wright and Boxer [37] for the corresponding pyro-derivatives lacking the $13^2$-$COOCH_3$-group. In case of Zn-pyro-Pheide-Mb, there are two high-field signals, I (−2.45 ppm) and II (∼−0.7 ppm), that are assigned to the methyl-groups of Val68 [37]. These signals are shifted in the spectra of Zn–Pheide–Mb (−2.35 and −1.0 ppm) and Zn–BPheide–Mb (−2.25 and −1.17 ppm). The high-field shifts are caused by the aromatic ring-current of the tetrapyrrole macrocycle, it therefore proves that both chlorophyll-derivatives are inserted into the heme pocket. The magnitude of the ring-current decreases in the order porphyrin > chlorin > bacteriochlorin [43]. The shift of peak I to lower field in the bacteriochlorin–Mb complex can be rationalized by this decreased ring-current. The opposite shift of peak II, from −1.0 to −1.17 ppm is probably related to the presence of the 3-acetyl-group, which is close to Val68. Similar relative shifts among the Mb complexes of the respective pyro-compounds, Zn–pyro-Pheide and Zn–pyro-BPheide, have been reported previously [37]. A still unexplained feature is the occurrence of satellite signals. In the spectrum of Zn–Pheide–Mb, these are clearly visible at the high-field side of both peaks, with an intensity ratio of 4:1 (Fig. 2). A similarly distinct splitting had been observed by Wright and Boxer [37] for the Mb-complex of Zn–Pyro-Pheide b, while Zn–pyro-Pheide-a–Mb only showed an unresolved shoulder in the peak at highest field. No such satellites

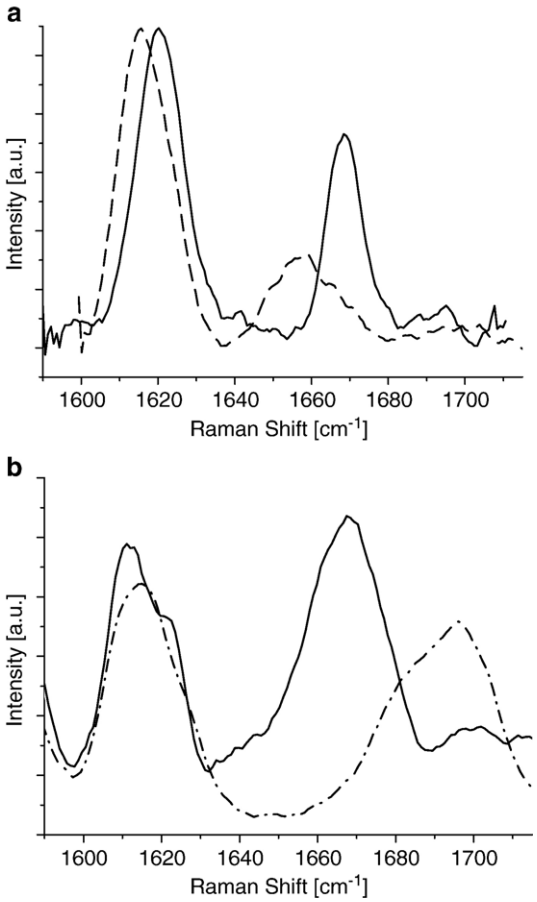


Fig. 7. Resonance Raman spectra (high frequency region) a) of Zn–BPheide–Mb (—) in NaPB (10 mM, pH 6.3) and free Zn–BPheide (–·–·–) in THF, and b) of Zn–Pheide–Mb (—) in NaPB (10 mM, pH 6.3) and free Zn–Pheide (–·–·–) in THF.

are seen in the spectrum of Zn–BPheide–Mb. The split signals reflect some heterogeneity in the sample on the NMR time-scale, which would then be reduced in Zn–BPheide–Mb, but the molecular basis remains unclear at present.

Further information on the binding situation was gained by comparing the low-temperature resonance Raman spectra of the Mb-pigment complexes with those of the free pigments in tetrahydrofuran (THF). In the higher frequency region, the resonance Raman spectrum of Zn–Bpheide and Zn–Pheide should contain a band in the 1600/1620 $cm^{-1}$ region, arising from the methine bridge stretching mode which is an indirect indicator of the Zn coordination [44]. In THF, where Zn is five coordinated, this band is observed at 1615 $cm^{-1}$ (Fig. 7), at a slightly higher position than previously reported at room temperature [44]. The shift can be due to changes in the solvent properties at low temperature, or to the fact that the molecule becomes more planar in the solvent at room temperature. In the Mb-complex of Zn–BPheide–Mb, the position of this band is 1620 $cm^{-1}$ and it unambiguously indicates that the central Zn is five coordinated [45]. In the spectrum of Zn–Pheide–Mb (1612 and 1622 $cm^{-1}$), this band is at slightly lower frequency (1612 instead of 1615 $cm^{-1}$), but still indicative of a single extra ligand. The lower frequency indicates that the ZnPheide is more

planar in its binding site that the Zn–Bpheide [46]. The shoulder appearing at 1622 $cm^{-1}$ in the spectrum of Zn–Pheide likely arises from the vinyl stretching mode of the molecule, as discussed by Feiler [46].

The acetyl and keto carbonyl stretching modes of Zn–Bpheide are expected to contribute in the 1620/1660 $cm^{-1}$ and 1660/1685 $cm^{-1}$ range, respectively [44], and their precise frequency depends on their involvement in intermolecular H-bonds. In the spectrum of Zn–Bpheide in THF, the band at 1657 $cm^{-1}$ can be assigned to the free acetyl carbonyl; this group is missing in the spectrum of Zn–Pheide. It is quite broad (25 $cm^{-1}$), indicating the presence of impurities capable of H-bonding interactions with this group in the THF, most likely some water. Under Raman resonance conditions, the contribution of the $13^1$ carbonyl group is expected to be weak (see, e.g., spectra in ref [46]). A very weak band near 1685 $cm^{-1}$ in Zn–Bpheide spectra is indeed observed, which arises from the stretching modes of the free $13^1$-keto carbonyl group. In the Mb-complex of Zn–BPheide, a very intense band is found at 1668 $cm^{-1}$, which is quite unusual for a carbonyl band. There are, however, no other strong bands in this complex between 1620 and 1668 $cm^{-1}$, where the stretching frequencies of the acetyl carbonyl are expected to contribute. We therefore assume that this band arises from the stretching frequencies of the acetyl carbonyl, which then must be free from interactions and in an apolar environment. This group is thus completely protected from the outside water solvent and must be embedded in the binding pocket. The fact that it is narrow indicates that all acetyl carbonyl groups share similar environments in terms of dielectric constant. The contribution of the keto carbonyl is difficult to detect in these spectra. A very weak band at 1685 $cm^{-1}$, slightly above the noise level, might be present in the spectrum of the Zn–BPheide–Mb complex. It is more likely, however, that a sizeable fraction of this group shows interactions and then contributes to the strong band at 1668 $cm^{-1}$. In the spectra of the Mb-complex of Zn–Pheide, the contribution of the keto carbonyl groups actually appears as a broad band centered at this frequency, indicating that these groups are involved in intermolecular interactions, likely with surrounding solvent.

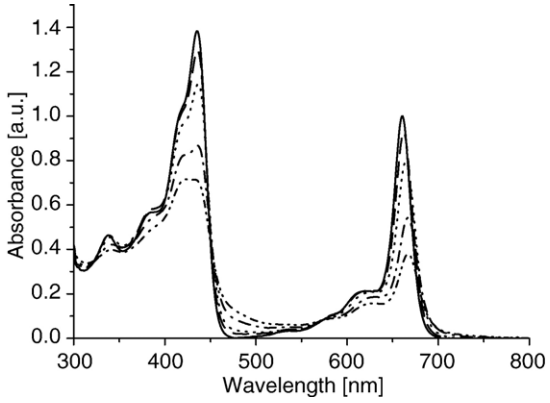


Fig. 8. Photobleaching reaction of Zn–Pheide–Mb in air. Absorption spectra before (—), and after 1 min (– – –), 3 min (····), 10 min (–·–·) and 20 min (–··–··) irradiation in Na-PB (10 mM, pH 6.3) containing pyridine (0.15%).

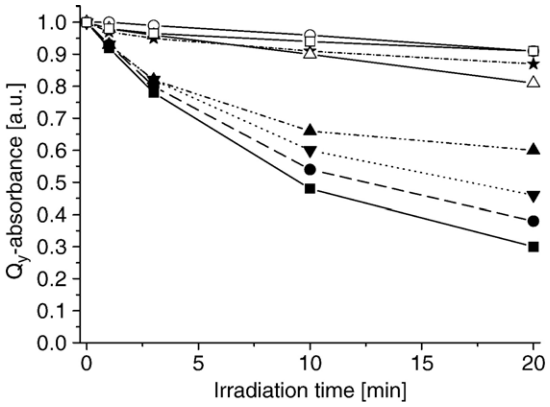


Fig. 9. Bleaching kinetics of the $Q_y$-absorption during irradiation of an aerobic solution of Zn–Pheide–Mb in NaPB (10 mM, pH 6.3) (■), the same solution containing pyridine (0.15%) (●), the same solution containing pyridine (0.15%) and β-carotene ($7.5\times10^{-6}$ M) (▼), Ar saturated solution containing pyridine (0.15%) (▲), and of free Zn–Pheide in aerobic NaPB (10 mM, pH 6.3) containing pyridine (0.15%) (★), in aerobic acetone (○), in aerobic methanol (□), and in aerobic toluene (△).

### 3.3. Photobleaching of Zn–Pheide–Mb and free Zn–Pheide

When a solution of Zn–Pheide–Mb in equilibrium with air is illuminated with red light ($\lambda \geq 630$ nm), the intensities of the Soret- and the $Q_y$-absorbance rapidly decrease (Fig. 8). In the $Q_y$-region, only 38% of the original intensity is left after 20 min illumination. At the same time the structure of the absorption spectrum changes significantly. In the Soret-region, the shoulder at 419 nm bleaches more slowly than the main band and both bands reach similar intensities after 20 min. The $Q_y$-band shifts from 661 to 667 nm and its red-wing broadens considerably. There are no new bands, but a general absorption increase in the region of 470 to 520 nm, without isosbestic points. The pigments remain bound to the protein during these transformations, which is proven by applying the irradiated, concentrated solution to a small column of Sephadex-G-25 (see reconstitution conditions). The complex moves as a single band, while free pigments are irreversibly bound to the stationary phase under these conditions. After subsequent standing in the dark, there are no back reactions of the irradiated complexes, the shape of the absorption spectrum and its intensities remain unaltered.

Photobleaching of Mb-bound Zn–Pheide, followed by the decrease of the $Q_y$-absorption, is considerably faster than that of free Zn–Pheide in solution, including the buffer system used for the reaction of the Mb complex (Fig. 9). In all solvents tested, the main spectral change is a reduction of the $Q_Y$ and the Soret bands. There is in particular no red-shift of the $Q_y$-band, and only in the case of toluene and NaPB (10 mM, pH 6.3) as solvent, there is an intensity increase in the region from 450 to 520 nm. In the latter case, 13% of the pigment are bleached ($Q_y$-band) after 20 min irradiation (Fig. 9). In order to dissolve Zn–Pheide in the buffer, 0.15% pyridine were added. While the addition of the same amount of pyridine reduced bleaching of the Mb-complex, it is still faster than that of the free pigment. Obviously, binding to Mb accelerates oxidative photobleaching of Zn–Pheide.

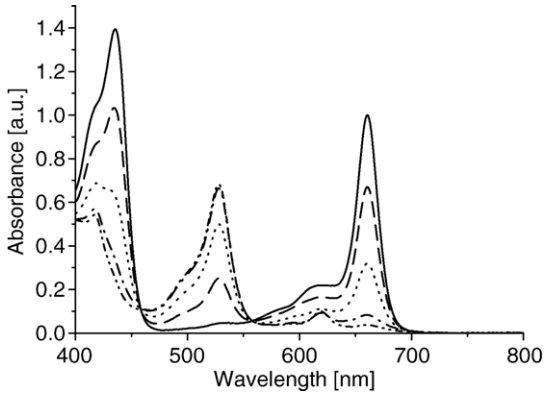


Fig. 10. Photoreaction of Zn–Pheide–Mb under Ar in the presence of sodium dithionite (0.3%). Absorption spectra before (—), and after 1 min (– – –), 3 min (····), after 10 min (–·–·) and 20 min (–··–··) irradiation in NaPB (10 mM, pH 6.3) containing pyridine (0.15%): the reaction follows the same scheme if no pyridine is added to the solution.

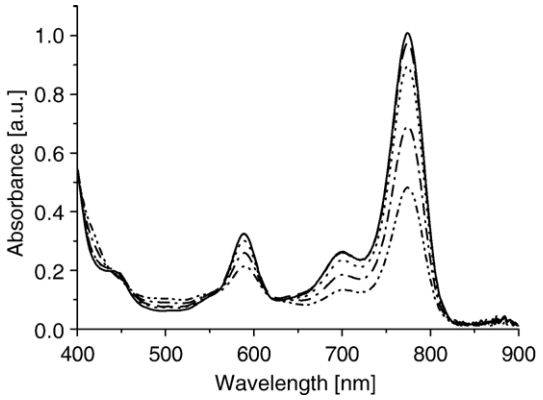


Fig. 12. Photoreaction of Zn–BPheide–Mb under Ar with Na-dithionite (0.3%). Absorption spectra before (—), and after 1 min (– – –), 3 min (····), 10 min (–·–·) and 20 min (–··–··) irradiation in NaPB (10 mM, pH 6.3) containing pyridine (0.15%).

In contrast to the free pigments, where bleaching is (almost) completely inhibited in a deaerated, Ar-saturated solution, Zn–Pheide–Mb still bleaches to approximately 40% during 20 min illumination (Fig. 9). No reliable experiments could be done with carotenes due to their poor solubility in aqueous solutions and the ensuing scattering, but the results shown in Fig. 9 indicate that β-carotene, too, is only partly effective in inhibiting the bleaching.

A different type of photoreaction is observed in the presence of a reductant. If sodium dithionite is added to an Ar-saturated solution of Zn–Pheide–Mb and the same irradiation protocol is applied, the intensity of the $Q_y$-band rapidly decreases and a new band rises at 528 nm, with two nearly isosbestic points at 458 and 557 nm (Fig. 10). Subsequent standing of the irradiated solution in the dark for 15 min with the reductant still present in the solution, results in a small recovery (7%) of the $Q_y$-band and a concomitant decrease of the new band at 528 nm. The recovery is much larger (~40%) when the irradiated solution is concentrated and purified over a small gel-filtration column. No pigment is retained on the column, and the solution turns successively green again, while the reductant is washed out. A large amount of the pigment(s) thus remains bound to the protein during the entire reduction and oxidation cycle. Qualitatively, the original absorption spectrum is nearly recovered (not shown), deviations are mainly due to the concomitant formation of a second, minor product with absorptions at 619 and 420 nm, probably due to dehydrogenation at C-17/18 [31].

A similar photoproduct is also formed reversibly in an aqueous solution of free Zn–Pheide ($\lambda_{max}$ = 529 nm), but again at a slower rate than with the Mb complex: Soret- and $Q_y$-bands decrease only by 40% and 30%, respectively. However, in this case, there is no obvious by-product as in the protein complex. In contrast to the Mb-complex, the reaction of free Zn–Pheide also continues in the dark with the reductant still present: after 15 min in the dark, an additional 4% of the $Q_y$-band is bleached, with a concomitant increase of the band at 529 nm.

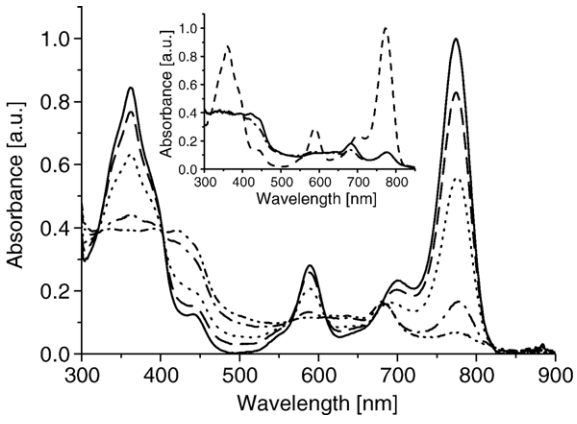


Fig. 11. Photobleaching reaction of Zn–BPheide–Mb in air. Absorption spectra before (—), and after 1 min (– – –), 3 min (····), 10 min (–·–·) and 20 min (–··–··) irradiation in NaPB (10 mM, pH 6.3) containing pyridine (0.15%). Insert: Absorption spectra of Zn–BPheide–Mb before (– – –) and after (–·–·) 10 min irradiation, and after 15 min standing in the dark (—).

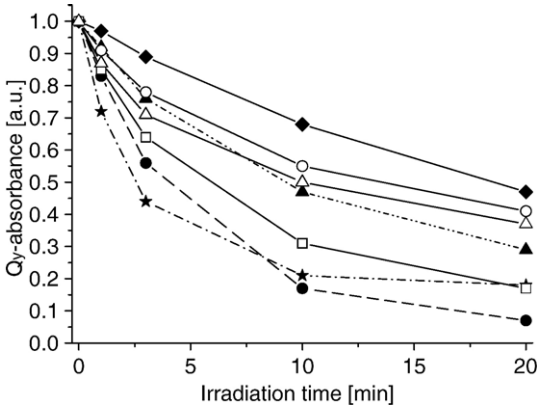


Fig. 13. Bleaching kinetics of the $Q_y$-absorption during irradiation of an aerobic solution of Zn–BPheide–Mb in NaPB (10 mM, pH 6.3) containing pyridine (0.15%) (●), the same, Ar saturated solution (▲), the same solution containing sodium dithionite (0.3%) (♦), and of free Zn–BPheide in aerobic NaPB (10 mM, pH 6.3) containing pyridine (0.15%) (★), in aerobic acetone (○), in aerobic methanol (□), and in aerobic toluene (△).

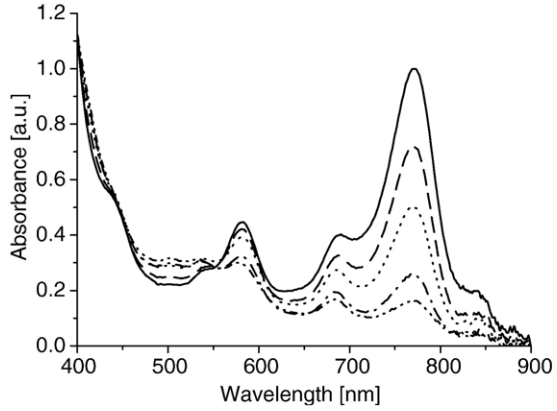


Fig. 14. Photoreaction of free Zn–BPheide under Ar in the presence of sodium dithionite (0.3%). Absorption spectra before (—), and after 1 min (– – –), after 3 min (····), after 10 min (–·–·) and after 20 min (–··–··) irradiation in NaPB (10 mM, pH 6.3) containing pyridine (0.15%).

### 3.4. Photobleaching of Zn–BPheide–Mb and free Zn–BPheide

When a solution of Zn–BPheide–Mb in buffer under aerobic conditions is irradiated with red light ($\lambda \geq 630$ nm), the intensities of the $Q_y$-, $Q_x$- and Soret bands decrease rapidly (Fig. 11). At the same time two new absorption bands are evolving, one around 681 and the other around 440 nm. These new bands are characteristic for chlorins like [3-acetyl]-Chl, which are easily formed by dehydrogenation of ring B in bacteriochlorins to the respective chlorins [47]. This dehydrogenation is in fact so rapid that some chlorin product is already formed during incorporation of Zn–BPheide into Mb: indications of these bands are present in the original spectrum (Fig. 11). In addition to this reaction, there is a broad absorption increase over most of the visible spectrum, without any pronounced features. As in the case of the Zn–Pheide complex, the reaction can only be partially inhibited by the exclusion of oxygen (70% bleaching in 20 min.). In both cases, there are no back reactions if the complexes are kept in the dark. If the illumination reaction is interrupted after 3 or 10 min, the bleaching and the evolution of the two new bands even continues in the dark over periods up to 15 min, viz. some product is formed which is capable of bleaching the pigment in the dark. This effect has also been obtained with free Zn–BPheide (see below).

If sodium dithionite is added to an Ar-saturated solution, the photobleaching is reduced, but there is no product formed which has a pronounced absorption in the visible region (Fig. 12). Solely in the region around 500 nm, a slight absorption increase is observed. Unfortunately, the strong background signal of dithionite solutions prevents spectroscopy at wavelengths <400 nm. Again, the pigments remain bound to the protein in all cases described, as verified by the chromatography assay.

Irradiation of free Zn–BPheide in buffer (NaPB, 10 mM, pH 6.3) or solvent results in comparable spectral changes as in the protein complex, Fig. 13 shows the associated $Q_y$-absorption intensity decreases. As shown in Fig. 14, the free pigment is far more sensitive to irradiation in the presence of sodium dithionite than the pigment in the protein complex, the very fast absorption decrease of the $Q_y$-band is not associated with any evolution of new bands.

### 3.5. Kinetics of Zn–BPheide related degradation

The bleaching kinetics are compared by following the decrease of the $Q_y$-absorption during irradiation (Fig. 13). As in the case of Zn–Pheide–Mb, the pigment protein complex undergoes the fastest photodegradation if irradiated in buffer in equilibrium with air. By degassing and saturating the solution with Ar, Zn–BPheide–Mb shows reduced photodegradation, but even under these conditions it bleaches to approximately 30% during 20 min illumination. There was no effect by addition of β-carotene, although this experiment is hampered by the poor solubility of the pigment. Only the addition of Na-dithionite can further reduce the bleaching. Generally, the kinetic differences between free and bound pigment are less, however, then with Zn–Pheide, because free Zn–BPheide undergoes a comparably faster photodegradation in buffer as well as in methanol. The photodegradation of the free chromophore depends on the solvent (methanol>toluene>acetone), but obviously, Zn–BPheide is significantly more sensitive to photobleaching than Zn–Pheide, whether bound to Mb or free.

### 3.6. HPLC analyses of photoproducts

Pigments were extracted from the protein complex and analyzed by HPLC (Fig. 4). The assignment of the different peaks was done by co-chromatography with authentic products, on the basis of identical retention times and identical in situ absorption spectra of the respective HPLC-peaks. Before irradiation, the major peak **a** ($t_r$=25.9 min), corresponding to $13^2$R-Zn–Pheide, is accompanied by two minor peaks (**b**, $t_r$=23.5 min and **c,** $t_r$=24.4 min). Pigment **b** was identified by its spectrum and co-chromatography as $13^2$S-OH-Zn–Pheide, which moves faster than the educt on the reverse-phase column due to its higher polarity. Its presence in the reaction mixture even before irradiation is due to the very easy formation of this compound, which occurs during the reconstitution or the extraction process. However, there is neither $13^2$S-Zn–Pheide nor $13^2$R-OH–Zn–Pheide present in the complex before irradiation. The identity of peak **c** remains ill defined at present. According to the absorption spectrum ($\lambda_{max}$=418 and 653 nm, intensity ratio $A_{Soret}/A_Q$=1.7), it is a chlorin. Its molecular weight was determined by mass spectroscopy to 686 g/mole. The mass difference to Zn–Pheide is 32 units, which corresponds to the mass of an $O_2$-molecule. The retention time of compound **c** lies between those of $13^2$S-OH–Zn–Pheide and $13^2$R-Zn–Pheide on the reverse phase column, this high polarity is in agreement with an oxygen-rich compound.

When Zn–Pheide–Mb had been irradiated for 20 min with red light ($\lambda \geq 630$ nm) in buffer in equilibrium with air, both peaks **b** and **c** are significantly increased relative to peak **a**, and a further product is formed (**d**, $t_r$=27.1 min, Fig. 4; the HPLC-traces are normalized to the intensity of peak **a** to compare the relative intensities of products **b**, **c** and **d** before and after irradiation). Peak **d** has been identified by co-chromatography and by its spectrum as Proto-Zn–Pheide [31]. It possesses an additional C-17/C-18 double bond (Fig. 1). The corresponding Mg-complex, Proto-Chlide, is a late biosynthetic intermediate in Chl formation [48]. Proto-Zn–Pheide is not present in the unirradiated complex, and is

formed only in traces if free Zn–Pheide is irradiated in buffer, acetone, methanol or toluene (chromatograms not shown). Thus, the same oxidation products are formed eventually, by irradiation of the free pigment and its Mb-complex.

HPLC analyses of the photooxidation products of Zn–BPheide–Mb (20 min irradiation in aerated buffer, Fig. 5) showed only one colored product (**b**, $t_r$=11.6 min) besides the educt, 13$^2$R-Zn–BPheide (peak **c**, $t_r$=12.9 min). It was identified as the well-known oxidation product, [3-acetyl]-13$^2$R–Zn–Pheide [47], by co-chromatography with authentic pigments. As in the case of dehydrogenation at the C17/C-18 bond (see above), this dehydrogenation at C7/C8 results in an increased retention time on the reverse phase column, corresponding to a lower polarity. The corresponding S-epimers (**b'** and **c'** in Fig. 5) are only found in traces before and after irradiation.

## 4. Discussion

### 4.1. Binding specificity

Protoheme is bound to Mb with rings A and B buried deeply in the hydrophobic interior, the central metal is ligated firmly to the proximal histidine H93 (numbering refers to sperm whale Mb) and weakly to the distal H64 which is replaced by $O_2$ in oxy-myoglobin [49]. Rings C and D are located more peripherally, with the two carboxyl groups at the surface and twisted out of the plane of the macrocycle in a distinct way: the propionic acid at C-13 bends down (α), if viewed as shown in Figs. 1 and 6, the one at C-17 bends up (β) and back to be H-bonded to H97. There is one crystal structure published with a different type of chromophore bound to Mb, viz. the open-chain tetrapyrrole, biliverdin (BV) [25]. This chromophore is present in the BV-Mb complex in a geometry that is very similar to that of protoheme, including in particular the conformation of the propionic acid side chains. In Chl and BChl, C-17 is chiral and the propionic acid side-chain faces up (β). The C-13 propionic acid of protoporphyrin is transformed during Chl biosynthesis: it is methylated and then becomes part of the isocyclic ring [50]. By virtue of the asymmetric C-13$^2$, the $COOCH_3$ substituent faces down (α). The orientation of the two side-chains is hence similar to that imposed by the protein on the achiral protoheme [49] and BV [25] in their Mb complexes. There is no published [37] structure of a Mb-complex with a chlorophyllous chromophore, but one can readily imagine that they fit well into the binding pocket: Chl and Fe-protoporphyrin have not only a similar overall structure, in particular at rings A and B, and central metals that are coordinatively unsaturated, but also a similar geometry of the propionic acid side chains. This provides a rationale for the ready formation of such complexes with (B)Chlides carrying a free 17-propionic acid side chain.

While the majority of (B)Chlides have the 13$^2$R,17S-configuration described above, minor amounts are present in organisms with a type I reaction center that have the 13$^2$S,17S-configuration [51–54]. These so-called prime-chlorophylls (Chl *a'*, Chl *d'*, BChl *g'*) are also readily formed after isolation of the pigments (see, e.g., [55]) and likely to arise during chemical modifications used to improve photodynamic action, as long as the enolizable β-ketoester system is retained. Binding has been studied of such isomers in which the 13$^2$-$COOCH_3$-group faces up (β). The results support a geometrical selection of Mb: there is not only a preference for the 13$^2$R-epimers (Zn–BPheide and Zn–Pheide), but the 13$^2$S-epimers also epimerize readily, such that Mb can be considered, in a very general sense, an epimerase. Known chlorophyll-binding proteins and the enzymes involved in Chl-biosynthesis are very selective with respect to the substituents and the stereochemistry at the isocyclic ring E, and it is currently not known which enzymes, if any, are responsible for the epimerization leading to the prime-pigments found in all type I reaction centers. The good correlation of the amount of, e.g., Chl a' and that of PSI suggests, however, a strict control [56]. The epimerization of Zn–(B)Pheide (13$^2$R) to Zn–(B)Pheide *a'* (13$^2$S) by apo-Mb could then indicate an alternative mechanism, whereby epimerization is accelerated by the binding site. Even though its direction is opposite to the one required for Chl a' generation; it may then be considered an example for an autocatalytic action of the binding site, where no additional epimerase would be required. Epimerization is known to be accelerated by acids as well as by bases. Presuming a similar insertion of the chlorophyllous derivatives and heme into the Mb binding pocket, potential candidates for such an effect were His-97 and Ser-92, which are close to the 13-propionic acid side chain of myoglobin [39].

Several modified pigments were used to further analyze the specificity of the binding site. The results summarized in Table 1 point to two important aspects: one sheds more light on the stereochemical restrictions discussed above, the other is the central metal. Additional substituents can be introduced at C-13$^2$, or the $COOCH_3$-group removed. The latter pigments have already been introduced early on [17], the lack of the 13$^2$-substituent obviously does not interfere with binding. This can be rationalized from the high-resolution X-ray structure of oxygenated Mb [49] (pdb entry 1A6M), where the 13$^3$ carboxyl group does not interact with any of the side chains and not even in an obvious way with localized water molecules, while the 17$^3$-carboxyl group is positioned such that H-bonding is possible with H97. Additional substituents at C-13$^2$ render this center "less asymmetric", as much as the spatial requirements of the 13$^2$-α and 13$^2$-β substituents are concerned. This situation has been studied with the stereoselectively 13$^2$S hydroxylated pigment, 13$^2$S–OH–Zn–Pheide, in which the 13$^2$-$COOCH_3$-substituent has the same geometry as in Chlide *a*, but the 13$^2$-H is replaced by the much larger OH. The pigment binding indicates that the OH-substituent at the β-face of ring E does not inhibit binding. However, in this case of two sterically more demanding chromophores even the epimer with the $COOCH_3$-group facing "up" is bound, and the steric selection is not very strong.

Variations of the central metal include (a) four examples (Mg, Zn, Fe and Ni), which are known to have an open binding site for (at least) a fifth ligand [28], (b) one (Pd) which does, in tetrapyrroles, not readily accept a fifth ligand [57,58], and c) two pheophorbides which lack the central metal. There is a clear bifurcation among these pigments: tetrapyrroles containing the four metals with open ligation sites bind to apo-Mb under the reconstitution conditions, while those containing Pd or no central metal do not bind. This is reminiscent of the selectivity of heme and (B)Chl binding sites that

can be manipulated by site-directed mutagenesis. Whenever there is a good ligand like histidine near the central metal, the site is occupied by a metalated tetrapyrrole, viz. a (B)Chl, and when there is a bulky amino acid instead that does not allow to carry in a ligand, the site will take a (B)Phe (see ref [59]).

Published data on the formation of Mb complexes with open-chain tetrapyrroles seem to contradict the selectivity for tetrapyrroles carrying a central metal with open ligation sites. Biliverdin (BV) and several other bilins have been incorporated successfully into apo-Mb (sperm-whale), and one member has been crystallized. Important features of the latter complex are the same orientation of the pigment with the two propionic acid side chains protruding from the pocket to the surface of the protein, and similar conformations of the C-8-substituent (corresponding to the C-13 substituent in heme) which is facing "down", and the C-12 substituent (corresponding to the C-17 substituent in heme) that is facing "up". In contrast to previously tested bile pigments [21], PCB showed no binding under similar conditions. This may be due to the use of a different Mb (horse heart instead of sperm whale), in combination with the rather rigid 3E-ethylidene substituent that is deeply buried in the Mb pocket. Interestingly, binding was recovered if the reconstitution was done in the presence of $Zn^{++}$. Under these conditions, a fluorescent chromophore is formed. Apparently, the chromophore is now bound as the Zn–PCB complex, which by virtue of the central metal is accepted to the binding site. In a similar way, Zn-chelation of the BV-sperm-whale-Mb-complex resulted in a complex of much higher stability as without chelation [23].

### 4.2. Photochemistry

Chlorophyll- and bacteriochlorophyll-derivatives have attracted considerable interest in photomedicine. Many of them are excellent sensitizers of reactive oxygen species by virtue of their long-lived excited states. The particular advantages and applications have been summarized recently [26,60–62]. Much less is known on the fate of these molecules in the body. They are rapidly excreted [63], but neither are the excretion products known, nor the involvement of light in the process.

Part of our interest in the photochemistry of chlorophyll derivatives [64–66] relates to the latter question, and to the role of the molecular environment in the process. Myoglobin has been chosen for this study as a model for monomeric pigments in the environment of a hydrophilic protein. In summary, the photoreactions of chlorophylls follow similar pathways in the Mb-complexes as in organic solvents. Under oxidizing conditions, there are dehydrogenations of the reduced rings to produce Chlides from BChlides, and protochlorophyllides from Chlides. It should be noted, that there is also bleaching to products absorbing only little in the visible spectral region, whose structures are currently unknown. In fact, these products represent, in solution, the majority of the bleached chlorophyll derivatives (Figs. 8, 11), which is indicated by the term "bleaching". A first attempt has recently been made to analyze the complex mixture of these color less products [67]. Under reducing conditions, chlorophyll-derivatives are subject to the Krasnovskii reaction [68], generating 10,20-dihydrochlorins with an absorption in the 530 nm range [69]. This reaction requires, apart from a reductant, the presence of a nucleophile like pyridine, $NH_3$ or histidine. The fact that the reduction also takes place in the protein complex, when no additional pyridine is added (see legend Fig. 10), supports the correct binding of the pigment in the binding pocket, where (one of) the two histidines H64 and H93 can act as the nucleophile.

Although many of the photoproducts are similar in Mb and in solution, if judged from their absorption spectra, the reaction kinetics differ: in general, the photoreactions are accelerated, and they also differ qualitatively in some details.

A particularly intriguing feature of the photooxidation of Zn–BPheide is that this reaction continues in the dark after turning off the light (Fig. 11). Reactions of this type have recently been described for carotenoids, where they have been attributed to the formation of carotenoid-peroxides [70]. The current finding of a reaction product with a mass increased by 32 μm over the educt, Zn–Pheide, raises the possibility that peroxides may be formed too, from chlorophylls in the light under aerobic conditions, and that they may be responsible for the continuing degradation in the dark.

The heme pocket of myoglobin provides a ligand to the heme: the proximal histidine H93 is bound firmly to the central metal from the top side (β) of the tetrapyrrole. There is also a second, distal histidine (H64) at the opposite side (α) that does not bind directly to the central metal, but rather lines a cavity which is accessible from the exterior and of functional significance: it provides enough space, in a moderately hydrophobic environment, for a molecule of $O_2$ to bind to the central metal, Fe. The requirements for binding $O_2$ to heme have been the subject of numerous studies [71]. There is much less known on the binding, if any, of $O_2$ to a central Mg in tetrapyrroles. We [67] and others [72] have obtained evidence, from a solvent study, that such complexes can be formed, possibly transiently; which can explain the rapid photo-autoxidation of chlorophylls in weakly ligating solvents, where $O_2$ binding can compete with that of the solvent [65]. The reduced photobleaching after addition of pyridine (Fig. 9) is yet another example: pyridine is an excellent ligand which out-competes $O_2$ from the site. The acceleration of photobleaching in the Mb complexes may then relate to a complementary mechanism. Here, the residence time of $O_2$ bound weakly to the central Zn, would be increased due to its binding-pocket having involved to assist $O_2$ binding. Such a mechanism would, last but not least, also be supported by the ongoing photobleaching under an inert atmosphere, where sufficient $O_2$ is retained even after repetitive degassing to allow for an ongoing, albeit slow photooxidation.

Falk et al. [23] have employed apo-Mb as a reaction vessel capable of modifying reaction pathways and selectivities. The epimerization and photoreaction data reported here support this notion. The Mb-binding-pocket seems to have a certain flexibility which allows its acting as an epimerase, or an enhancement of $O_2$-dependent photoreactions and base-dependent photoreductions. Further studies are underway to shed more light on protein pigment interactions in other artificial Chl–protein systems.

## Acknowledgements

Work was supported by the Deutsche Forschungsgemeinschaft (SFB 533, TP A6). We thank Marcin Krajewski for the measurement of the NMR-spectra and his helpful advice during analyses, George Wiegand for sedimentation studies, Wolfgang Reuter for his introduction into preparative gel electrophoresis, and Bernhard Granvogl for the measurement of the mass spectra and their evaluation.

## References

[1] R.E. Dickerson, J.C. Kendrew, B.E. Strandberg, The crystal structure of myoglobin: phase determination to a resolution of 2 A. by the method of isomorphous replacement, Acta Crystallogr. 14 (1961) 1188–1195.
[2] M.F. Perutz, H. Muirhead, J.M. Cox, L.C.G. Goaman, Three-dimensional Fourier synthesis of horse oxyhemoglobin at 2.8 A. resolution: the atomic model, Nature 219 (1968) 131–139.
[3] I. Schlichting, K. Chu, Trapping intermediates in the crystal: ligand binding to myoglobin, Curr. Opin. Struck. Biol. 10 (2000) 744–752.
[4] J. Frank, I. Schlichting, Special issue: time-resolved imaging of macromolecular processes and interactions, J. Struct. Biol. 147 (3) (2004).
[5] A. Ostermann, R. Waschipky, F.G. Parak, G.U. Nienhaus, Ligand binding and conformational motions in myoglobin, Nature 404 (2000) 205–208.
[6] M. Schmidt, S. Rajagopal, Z. Ren, K. Moffat, Application of singular value decomposition to the analysis of time-resolved macromolecular X-ray data, Biophys. J. 84 (2003) 2112–2129.
[7] V. Srajer, T. Teng, T. Ursby, B. Perman, D. Bourgeois, C. Pradervand, F. Schotte, R. Kort, Z. Ren, W. Royer, K. Hellingwerf, M. Wulff, K Moffat, NS time-resolved X-ray diffraction studies of structural changes in biological macromolecules. Book of Abstracts, 216th ACS National Meeting, Boston, August 23–27, PHYS-390 (1998).
[8] X. Chen, B.M. Discher, D.L. Pilloud, B.R. Gibney, C.C. Moser, P.L. Dutton, De novo design of a cytochrome b maquette for electron transfer and coupled reactions on electrodes, J. Phys. Chem., B 106 (2002) 617–624.
[9] D.E. Robertson, R.S. Farid, C.C. Moser, J.L. Urbauer, S.E. Mulholland, R. Pidikiti, J.D. Lear, A.J. Wand, W.F. Degrado, P.L. Dutton, Design and synthesis of multi-haem proteins, Nature 368 (1994) 425–431.
[10] H.K. Rau, W. Haehnel, Design, synthesis, and properties of a novel cytochrome b model, J. Am. Chem. Soc. 120 (1998) 468–476.
[11] H. Frauenfelder, S.G. Sligar, P.G. Wolynes, The energy landscapes and motions of proteins, Science (1991) 1598–1603.
[12] F.G. Parak, Proteins in action: the physics of structural fluctuations and conformational changes, Curr. Opin. Struck. Biol. 13 (2003) 552–557.
[13] J. Schlichter, J. Friedrich, M. Parbel, H. Scheer, New concepts in spectral diffusion physics of proteins, Photonics Sci. News 6 (2000) 100–111.
[14] J.J. Katz, L.L. Shipman, T.M. Cotton, T.R. Janson, Chlorophyll aggregation: coordination interactions in Chlorophyll monomers, dimers and oligomers, in: D. Dolphin (Ed.), The Porphyrins, Academic Press, New York, 1978, pp. 402–458, Vol.
[15] V.V. Ponkratov, J. Friedrich, D. Markovic, H. Scheer, J.M. Vanderkooi, Spectral diffusion experiment with a denatured protein, J. Phys. Chem., B 108 (2004) 1109–1114.
[16] R.S. Moog, A. Kuki, M.D. Fayer, S.G. Boxer, Excitation transport and trapping in a synthetic Chlorophyllide substituted hemoglobin: orientation of the Chlorophyll S1 transition dipole, Biochemistry 23 (1984) 1564–1571.
[17] S.G. Boxer, A. Kuki, K.A. Wright, B.A. Katz, N. Xuong, Oriented properties of the chlorophylls—Electronic absorption-spectroscopy of orthorhombic pyrochlorophyllide alpha-apomyglobin single-crystals, Proc. Natl. Acad. Sci. U.S.A. 79 (1982) 1121–1125.
[18] R.M. Pearlstein, R.C. Davis, S.L. Ditson, Giant circular dichroism of high molecular-weight chlorophyllide–apomyoglobin complexes, Proc. Natl. Acad. Sci. U.S.A. 79 (1982) 400–402.
[19] R.C. Davis, R.M. Pearlstein, Chlorophyllin–apomyoglobin complexes, Nature 280 (1979) 413–415.
[20] H. Marko, N. Müller, H. Falk, Complex formation between biliverdin and apomyoglobin, Monatsh. Chem. 120 (1989) 591–595.
[21] G. Blauer, Complexes of bilirubin with proteins, Biochim. Biophys. Acta 884 (1986) 602–604.
[22] H. Falk, H. Marko, N. Muller, W. Schmitzberger, H. Stumpe, Reconstitution of apomyoglobin with bile pigments, Monatsh. Chem. 121 (1990) 893–901.
[23] H. Falk, H. Marko, N. Muller, W. Schmitzberger, The apomyoglobin heme pocket as a reaction vessel in bile pigment chemistry, Monatsh. Chem. 121 (1990) 903–908.
[24] H. Marko, N. Müller, H. Falk, Nuclear-magnetic-resonance investigations of the biliverdin–apomyoglobin complex, Eur. J. Biochem. 193 (1990) 573–580.
[25] U.G. Wagner, N. Müller, W. Schmitzberger, H. Falk, C. Kratky, Structure determination of the biliverdin apomyoglobin complex: crystal structure analysis of two crystal forms at 1.4 and 1.5 A resolution, J. Mol. Biol. 247 (1995) 326–337.
[26] J.G. Moser (Ed.), Photodynamic Tumor Therapy: 2nd and 3rd Generation Photosensitizers, OPA, Amsterdam, 1998.
[27] A. Struck, Chemisch modifizierte Bakteriochlorophylle und -Phäophytine. in den B Bindungsstellen$_{BA}$. H$_{A,B}$ von Photosynthetischen Reaktionszentren aus *Rhodobacter sphaeroides* R26: Pigmentsynthese, Pigmentaustausch und Spektroskopie., Dissertation, Universität München (1990).
[28] G. Hartwich, L. Fiedor, I. Simonin, E. Cmiel, W. Schaefer, D. Noy, A. Scherz, H. Scheer, Metal-substituted bacteriochlorophylls. 1. Preparation and influence of metal and coordination on spectra, J. Am. Chem. Soc. 120 (1998) 3675–3683.
[29] T. Omata, N. Murata, Preparation of chlorophyll a, chlorophyll b and bacteriochlorophyll a by column chromatography with DEAE-Sepharose CL-6B and Sepharose CL-6B, Plant Cell Physiol. 24 (1983) 1093–1100.
[30] M. Helfrich, Chemische Modifikation Von Chlorophyll-Vorstufen und Deren Verwendung zur Charakterisierung von Enzymen der Chlorophyll-Biosynthese, Dissertation, Ludwig-Maximilians-Universität, Munchen, 1995.
[31] M. Helfrich, S. Schoch, W. Schäfer, M. Ryberg, W. Rudiger, Absolute configuration of protochlorophyllide alpha and substrate specificity of NADPH-protochlorophyllide oxidoreductase, J. Am. Chem. Soc 118 (1996) 2606–2611.
[32] P.M. Schaber, J.E. Hunt, R. Fries, J.J. Katz, High-performance liquid-chromatography study of the Chlorophyll allomerization reaction, J. Chromatogr. 316 (1984) 25–41.
[33] A. Struck, H. Scheer, Modified reaction centers from *Rhodobacter sphaeroides* R26. 1. Exchange of monomeric bacteriochlorophyll with 13$^2$-hydroxy-bacteriochlorophyll, FEBS Lett. 261 (1990) 385–388.
[34] L. Fiedor, Modified Chlorophylls As Models for Primary Photosynthesis and Photosensitizers for Photodynamic Therapy of Cancer., Dissertation, Weizmann Institute of Science, Rehovot, 1994.
[35] M. Storf, A. Parbel, M. Meyer, B. Strohmann, H. Scheer, M. Deng, M. Zheng, M. Zhou, K. Zhao, Chromophore attachment to biliproteins: Specificity of PecE/PecF, a lyase/isomerase for the photoactive 3$^1$-Cysá84-phycoviolobilin chromophore of phycoerythrocyanin, Biochemistry 40 (2001) 12444–12456.
[36] F.W.J. Teale, Cleavage of the haem-protein link by acid methylethlyketone, Biochim. Biophys. Acta 35 (1959) 543.
[37] K.A. Wright, S.G. Boxer, Solution properties and synthetic chlorophyllide–apomyoglobin and bacteriochlorophyllide–apomyoglobin complexes, Biochemistry 20 (1981) 7546–7556.
[38] H. Mazaki, T. Watanabe, Self-catalyzed epimerization of Chlorophyll a/a' in organic solvents, Biochim. Biophys. Acta 1016 (1990) 190–196.
[39] R. Maurus, R. Bogumil, N.T. Nguyen, A.G. Mauk, G. Brayer, Structural and spectroscopic studies of azide complexes of horse heart myoglobin and the His-64 → Thr variant, Biochem. J. 332 (1998) 67–74.
[40] S.G. Boxer, K.A. Wright, Preparation and properties of a chlorophyllide–apomyoglobin complex, J. Am. Chem. Soc 101 (1979) 6791–6794.
[41] H. Snigula, (Bacterio)Chlorophyll-Modifikationen zur Einlagerung in Synthetische Peptide, Dissertation, Ludwig-Maximilians-Universität, Munchen, 2004.
[42] H. Falk, The Chemistry of Linear Oligopyrroles and Bile Pigments, Springer, Wien, New York, 1989.
[43] H. Scheer, J.J. Katz, Nuclear magnetic resonance spectroscopy of

porphyrins and metalloporphyrins, in: K.M. Smith (Ed.), Porphyrins and Metalloporphyrins, Elsevier, New York, 1975, pp. 399–524.
[44] A. Näveke, K. Lapouge, J.N. Sturgis, G. Harwich, I. Simonin, H. Scheer, B. Robert, Resonance Raman spectroscopy of metal-substituted bacteriochlorophylls: characterization of Raman bands sensitive to bacteriochlorin conformation, J. Raman Spectrosc. 28 (1997) 599–604.
[45] K. Lapouge, A. Näveke, J.N. Sturgis, G. Hartwich, D. Renaud, I. Simonin, M. Lutz, H. Scheer, B. Robert, Non-bonding molecular factors influencing the stretching wavenumbers of the conjugated carbonyl groups of bacteriochlorophyll a, J. Raman Spectrosc. 29 (1998) 977–981.
[46] U. Feiler, T. Mattioli, I. Katheder, H. Scheer, M. Lutz, B. Robert, Effects of vinyl substitutions on resonance Raman spectra of (Bacterio)chlorophylls, J. Raman Spectrosc. 25 (1994) 365–370.
[47] J.R.L. Smith, M. Calvin, Studies on the chemical and photochemical oxidation of Bacteriochlorophyll, J. Am. Chem. Soc. 88 (1966) 4500–4506.
[48] W.T. Griffiths, Protochlorophyllide Photoreduction, in: H. Scheer (Ed.), Chlorophylls, CRC-Press, Boca Raton, 1991, pp. 433–450.
[49] J. Vojtechovsky, K. Chu, J. Berendzen, R.M. Sweet, I. Schlichting, Crystal structures of myoglobin–ligand complexes at near-atomic resolution, Biophys. J. 77 (1999) 2153–2174.
[50] D.W. Bollivar, Intermediate steps in chlorophyll biosynthesis: methylation and cyclization, in: K.M. Kadish, K.M. Smith, R. Guilard (Eds.), The Porphyrin Handbook, Chlorophylls and Bilins: Biosynthesis, Synthesis and Degradation, vol. 13, Academic press, Amsterdam, 2002, pp. 49–70.
[51] M. Akiyama, H. Miyashita, H. Kise, T. Watanabe, S. Miyachi, M. Kobayashi, Detection of chlorophyll d' and pheophytin a in a chlorophyll d- dominating oxygenic photosynthetic prokaryote *Acaryochloris marina*, Anal. Sci. 17 (2001) 205–208.
[52] H. Maeda, T. Watanabe, M. Kobayashi, I. Ikegami, Presence of two Chlorophyll a' I. Molecules at the core of photosystem, Biochim. Biophys. Acta 1099 (1992) 74–80.
[53] M. Kobayashi, E.J. Vandemeent, C. Erkelens, J. Amesz, I. Ikegami, T. Watanabe, Bacteriochlorophyll g epimer as a possible reaction center component of Heliobacteria, Biochim. Biophys. Acta 1057 (1991) 89–96.
[54] P. Jordan, P. Fromme, H.T. Witt, O. Klukas, W. Saenger, N. Krauss, Three-dimensional structure of cyanobacterial photosystem I at 2.5A resolution, Nature 411 (2001) 909–917.
[55] H. Mazaki, T. Watanabe, T. Takahashi, A. Struck, H. Scheer, Epimerization of chlorophyll derivatives. V. Effects of the central magnesium and ring substituents on the epimerization of chlorophyll derivatives, Bull. Chem. Soc. Jpn. 65 (1992) 3080–3087.
[56] A. Nakamura, M. Akai, E. Yoshida, T. Taki, T. Watanabe, Reversed-phase HPLC determination of chlorophyll a' and phylloquinone in Photosystem I of oxygenic photosynthetic organisms. Universal existence of one chlorophyll a' I. molecule in Photosystem, Eur. J. Biochem. 270 (2003) 2446–2458.
[57] J.W. Buchler, Static coordination chemistry of metalloporphyrins, in: K.M. Smith (Ed.), Porphyrins and Metalloporphyrins, Elsevier, Amsterdam, 1975, pp. 157–232.
[58] A.M. Stolzenberg, L.J. Schussel, J.S. Summers, B.M. Foxman, J.L. Petersen, Structures of the homologous series of square-planar metallotetrapyrroles palladium(II) octaethylporphyrin, palladium(II) trans-octaethylchlorin, and palladium(II) tct-octaethylisobacteriochlorin, Inorg. Chem. 31 (1992) 1678–1686.
[59] C. Kirmaier, D. Gaul, R. Debey, D. Holten, C.C. Schenck, Charge separation in a reaction center incorporating bacteriochlorophyll for photoactive bacteriopheophytin, Science 251 (1991) 922–927.
[60] A. Brandis, Y. Salomon, and A. Scherz, Chlorophyll sensitizers in photodynamic therapy, in: Chlorophylls and Bacteriochlorophylls: Biochemistry, Biophysics, Functions and Applications in: B. Grimm, Porra R., Rudiger, W. Rüdiger, H. Scheer Springer, Berlin, 2006, pp. 461–483.
[61] A. Brandis, Y. Salomon, A. Scherz, Bacteriochlorophyll sensitizers in photodynamic therapy, in: Chlorophylls and Bacteriochlorophylls: Biochemistry, Biophysics, Functions and Applications (B. Grimm, R. Porra, W. Rüdiger, H. Scheer, (Eds.), Springer, Berlin, 2006, pp. 485–494.
[62] J.D. Spikes, J.C. Bommer, Chlorophyll and related pigments as photosensitizers in biology and medicine, in: H. Scheer (Ed.), Chlorophylls, CRC Press, Boca Raton, FL, 1991, pp. 1181–1204.
[63] V. Rosenbach-Belkin, L. Chen, L. Fiedor, I. Tregub, F. Pavlotsky, V. Brumfeld, Y. Salomon, A. Scherz, Serine conjugates of chlorophyll and bacteriochlorophyll: photocytotoxicity in vitro and tissue distribution in mice bearing melanoma tumors, Photochem. Photobiol. 64 (1996) 174–181.
[64] I. Tregub, S. Schoch, S. Erazo, H. Scheer, Red-light induced photoreactions of chlorophyll a mixtures with all *trans*- or 9-*cis*-β-carotene, J. Photochem. Photobiol. C 98 (1996) 51–58.
[65] J. Fiedor, L. Fiedor, N. Kammhuber, A. Scherz, H. Scheer, Photodynamics of the bacteriochlorophyll–caroteinoid system. 2. Influence of central metal, solvent and β-carotene on photobleaching of bacteriochlorophyll derivatives, Photochem. Photobiol. 76 (2002) 145–152.
[66] J. Fiedor, L. Fiedor, J. Winkler, A. Scherz, H. Scheer, Photodynamics of the bacteriochlorophyll–caroteinoid system. 1. Bacteriochlorophyll-photosensitized oxygenation of β-carotene in acetone, Photochem. Photobiol. 74 (2001) 64–71.
[67] L. Limantara, P. Köhler, B. Wilhelm, R.J. Porra, H. Scheer, Photostability of Bacteriochlorophyll a and Derivatives Used as Sensitizers for Photodynamic Tumor Therapy. Photochem. Photobiol. ISSN 0031–8655 (Print).
[68] A.A. Krasnovskii, Reversible photochemical reduction of chlorophyll by ascorbic acid, Dokl. Akad. Nauk SSSR 60 (1948) 421–424.
[69] H. Scheer, J.J. Katz, Structure of the Krasnovskii photoreduction product of chlorophyll *a*, Proc. Natl. Acad. Sci. U.S.A. 71 (1974) 1626–1629.
[70] J. Fiedor, L. Fiedor, R. Haessner, H. Scheer, Stable mono- and di-endoperoxides of β-carotene as products of photosensitized oxygenation, Biochim. Biophys. Acta 1709 (2005) 1–4.
[71] J.P. Collman, X. Zhang, Functional analogs of the oxygen binding and activating heme proteins, Comprehensive Supramolecular Chemistry, vol. 5, 1996, pp. 1–32.
[72] A. Drzewiecka-Matuszek, A. Skalna, A. Karocki, G. Stochel, L. Fiedor, Effects of heavy central metal on the ground and excited states of chlorophyll, J. Biol. Inorg. Chem. 10 (2005) 453–462.
[73] G.P. Moss, IUPAC-IUB Joint commission biochemical nomenclature (JCBN). Nomenclature of Tetrapyrroles. Recommendation 1986, Eur. J. Biochem. 178 (1988) 277–328.